

Regional Differences in Amyloid Deposition between ¹¹C-PiB PET Positive Patients with and without Elevated Striatal Amyloid Uptake

Franziska T Scheiwein^{1,2}, Kazunari Ishii^{1,3,4}, Chisa Hosokawa^{1,4}, Hayato Kaida¹, Tomoko Hyodo¹, Kohei Hanaoka⁴, Matthias Brendel², Peter Bartenstein², Axel Rominger^{2*} and Takamichi Murakami¹

¹Department of Radiology, Kindai University Faculty of Medicine, Osakasayama, Osaka, Japan

²Department of Nuclear Medicine, Ludwig-Maximilians-University of Munich, Munich, Germany

³Neurocognitive Disorders Center, Kindai University Hospital, Osakasayama, Osaka, Japan

⁴Division of Positron Emission Tomography, Institute of Advanced Clinical Medicine, Kindai University, Osakasayama, Osaka, Japan

Abstract

Purpose: In subjects showing an increased level of ¹¹C-Pittsburgh compound B (PiB) in positron emission tomography (PET) imaging of the brain, two groups can be distinguished: those with and without elevated PiB uptake in the striatum. We examined regional PiB uptake differences between these groups, and additionally compared them with PiB-negative subjects.

Methods: This study included 141 subjects complaining of cognitive impairment. Their clinical diagnoses were Alzheimer's disease (AD), mild cognitive impairment, dementia with Lewy bodies, frontotemporal lobar degeneration, or subjective cognitive impairment. PiB and ¹⁸F-fluorodeoxy-D-glucose (FDG) PET were performed in all subjects. PiB PET images were visually classified into three groups: 1) PiB-positive with uptake in any region of the cortex accompanied by striatal PiB uptake (STR_{POS}), 2) PiB-positive with cortical uptake but without striatal PiB uptake (STR_{NEG}), and 3) both cortex and striatum PiB-negative (PiB_{NEG}).

Standardised uptake value ratios (SUVR) and regional differences in PiB uptake were evaluated using voxel-based analysis of PiB and FDG uptake images.

Results: Eighty subjects were visually rated as PiB-positive: 11 had no increased PiB uptake in the striatal area, while 69 showed an elevated striatal PiB level. Sixty-one subjects were PiB-negative. Mean cortical SUVR was 1.46 ± 0.23 for STR_{NEG}, 2.00 ± 0.44 for STR_{POS} and 0.99 ± 0.19 for PiB_{NEG}. Apart from the striatum, PiB accumulation in the medial orbitofrontal cortex of STR_{POS} subjects was higher than in STR_{NEG} subjects. No significant differences in regional FDG distribution were observed.

Conclusion: PiB-positive cases with high striatal PiB uptake have an increased mean cortical SUVR in comparison to PiB-positive subjects without striatal uptake. This difference is most distinctive in the orbitofrontal cortex. We conclude that a high amyloid load in the striatum is linked to amyloid deposition occurring mostly in the frontal region, and may occur later in the course of AD progression.

Keywords: Dementia; Alzheimer's disease; ¹¹C-PiB-PET; FDG-PET; Amyloid deposit; Striatum

Introduction

Alzheimer's disease (AD) constitutes the most common form of dementia. As its prevalence increases with age, it imposes a substantial burden on societies with rising life expectancy [1,2]. Effective tools for accurate diagnosis and staging of the disease are needed to validate new therapeutic interventions; on the one hand for precise inclusion criteria and on the other hand for the assessment of treatment efficacy. Extracellular β -Amyloid plaques, neurofibrillary tangles of hyperphosphorylated tau and cerebral neuronal loss, constitute the neuropathological characteristics of AD. Biomarkers such as positron emission tomography (PET) of amyloid levels and cerebrospinal fluid assays offer feasible tools for the depiction of changes occurring in the pathophysiological progress of AD. The National Institutes of Aging and the Alzheimer's Association have recommended their use as clinical and research criteria for the diagnosis of AD [3,4]. ¹¹C-PiB, the first and most commonly used PET amyloid tracer, permits robust differentiation of AD patients and healthy controls, while regional PiB binding corresponds well with the findings of histopathological assays [5-9]. β -Amyloid plaques and tangles probably precede the onset of clinical symptoms by many years and show a typical distribution pattern in the cerebral grey matter during the progress of the disease [10-12]. Amyloid deposition typically starts in the basal frontal and temporal

lobes, before increasing and spreading to adjacent frontal, parietal, temporal, and occipital association cortices, as well as the hippocampal formation, which tends to be less strongly affected. Over time, deposits are seen in all cortical areas, including the primary neocortices. Later stages of AD show the involvement of not only isocortical structures, but also subcortical structures, such as the striatum, the thalamus, and the hypothalamus [10,13,14].

With regard to the PiB uptake in the striatal area, we have observed in our clinical and research work that amongst subjects with globally elevated PiB deposition, some subjects simultaneously showed increased tracer binding in the striata, while others did not. In this study, we aimed to investigate differences in global cortical PiB uptake, brain glucose

*Corresponding author: Axel Rominger, Department of Nuclear Medicine, Ludwig-Maximilians-University of Munich, Marchioninstr, 15D-81377 Munich, Germany, Tel: +49 89 4400 74650; E-mail: axel.rominger@med.uni-muenchen.de

Received March 13, 2017; Accepted March 28, 2017; Published April 04, 2017

Citation: Scheiwein FT, Ishii K, Hosokawa C, Kaida H, Hyodo T, et al. (2017) Regional Differences in Amyloid Deposition between ¹¹C-PiB PET Positive Patients with and without Elevated Striatal Amyloid Uptake. J Alzheimers Dis Parkinsonism 7: 317. doi: [10.4172/2161-0460.1000317](https://doi.org/10.4172/2161-0460.1000317)

Copyright: © 2017 Scheiwein FT, et al. This is an open-access article distributed under the terms of the Creative Commons Attribution License, which permits unrestricted use, distribution, and reproduction in any medium, provided the original author and source are credited.

metabolism, and clinical presentation in these two groups and PiB negative subjects.

Materials and Methods

Subjects

This study included 141 subjects who had complained of objective or subjective impairment, which predominantly involved a loss of memory. The population consisted of 71 women and 69 men with a mean age of 70.1 ± 9.8 years and a score of 23.3 ± 4.9 on the Mini-mental State Examination (MMSE). The subjects underwent ¹¹C-PiB PET and ¹⁸F-fluoro-2-deoxy-D-glucose (FDG) PET between May 2011 and May 2015, at the Institute of Advanced Clinical Medicine, Kindai University Hospital, Osakasayama, Osaka, Japan. The subjects were classified into PiB-positive (n=80) and PiB-negative (n=61) groups according to the visual read-out of their PiB images (Figure 1). The PiB-positive subjects were further classified as either striatal PiB positive (STR_{POS}) or striatal PiB negative (STR_{NEG}). The PiB positive subjects had the following clinical diagnoses: AD (n=39), mild cognitive impairment (MCI; n=36; 34 of whom were diagnosed with MCI due to AD and 2 with MCI due to dementia with Lewy bodies; DLB), DLB (n=4), and subjective cognitive impairment (SCI; n=1). The diagnoses of the PiB negative group were: AD (n=6), MCI (n=24), DLB (n=7), frontotemporal lobe degeneration (FTLD; n=7), SCI (n=11), and 6 with other non-dementia related diagnoses (1 with depression, 1 with anxiety neurosis, 1 with epilepsy, 1 with an alcohol-related disorder, and 2 undiagnosed). The diagnostic criteria of the Neurological and Communicative Disorders and Stroke-Alzheimer's Disease and Related Disorders Association (NINCDS/ADRDA) for AD and those of the third report of the Dementia with Lewy Bodies Consortium for DLB [15] were applied. Patients with MCI and FTLD met the published criteria [16-18]. This study was approved by our institution's ethical committee and all patients or guardians gave written informed consent prior to the inclusion of subjects into the study.

Data acquisition

Data acquisition of ¹¹C-PiB PET and ¹⁸F-FDG PET followed that described in a previous study [19]. Briefly, PET scans were performed using a PET scanner (ECAT Accel, Siemens AG, Erlangen, Germany) in the 3-dimensional mode. For ¹¹C-PiB PET, data were continuously acquired for 70 min after intravenous administration of 555 ± 185 MBq of ¹¹C-PiB. For ¹⁸F-FDG PET, a 30 min emission scan was acquired, starting 30 min after an intravenous injection of 185 MBq of ¹⁸F-FDG. The subjects underwent FDG PET within one month (before or after) of the PiB PET scanning.

Image processing

PiB-PET images were reconstructed from the data acquired 50–70

min after injection. In a first step, the PiB PET images of all subjects were visually assessed by two experienced nuclear medicine physicians blinded to the clinical information. This was performed on a workstation allowing individual adjustment of the window settings of the images. If the two ratings were inconsistent, a consensus was achieved by discussion. PiB positivity was evaluated in four cortical regions, including bilateral frontal, parietal, and temporal lobes (neocortical association areas), and bilateral precuneus/posterior cingulate gyri. PiB-positive images were defined as those having higher accumulation in the cerebral cortex than in the white matter (non-specific accumulation area [20]) and PiB-negative images were defined as those having no cortical accumulation. Those cases in which cortical PiB accumulation was suspected, but did not exceed the cerebral white matter binding, were rated as PiB equivocal cases and excluded from this study. In addition to the visual reading, an automated quantitative analysis was performed as follows: all of the PiB PET images were co-registered to the individual FDG PET images using statistical parametric mapping (SPM8, Wellcome Trust Centre for Neuroimaging, University College London, UK). The FDG PET images were then spatially normalised to the Montreal Neurological Institute (MNI) standard-space brain template, and the co-registered PiB PET images were also transformed to MNI space using the individual parameters obtained from the FDG PET normalisation. Using a template of the volumes of interest (frontal, parieto-temporal, precuneus/posterior cingulate and cerebellar cortex) set in MNI space, the SUV was measured for a composite cortex VOI. The standard uptake value ratios (SUVR) were then calculated relative to the SUV of the cerebellar cortex VOI for PiB, and relative to that of the pons for FDG.

In a second step, the PiB positive scans were classified as either striatal PiB positive (STR_{POS}) or striatal PiB negative (STR_{NEG}). Striatal uptake equalling or exceeding thalamic uptake was rated as positive. This visual assessment was performed by two independent readers blinded to the clinical information. As for the rating of global PiB positivity/negativity, a consensus was achieved by discussion if the two ratings were not concordant. Moreover, the striatal PiB uptake was calculated using a template VOI, and the mean SUVR of bilateral striata was created using the cerebellar cortex as a reference region.

We investigated the relationships of the visual findings with semi-quantitative values of ¹¹C-PiB PET, the regional PiB distribution pattern, the MMSE scores, and clinical and FDG PET findings. Additionally, voxel-wise analyses were performed as follows: all the anatomically standardized FDG-PET and PiB-PET images were smoothed with an isotropic 12 mm Gaussian kernel to increase the signal-to-noise ratio and to compensate for differences in gyral anatomy between individuals. The individual FDG image counts were compared with covariates of pontine FDG uptake counts. In the PiB analyses, the individual PiB

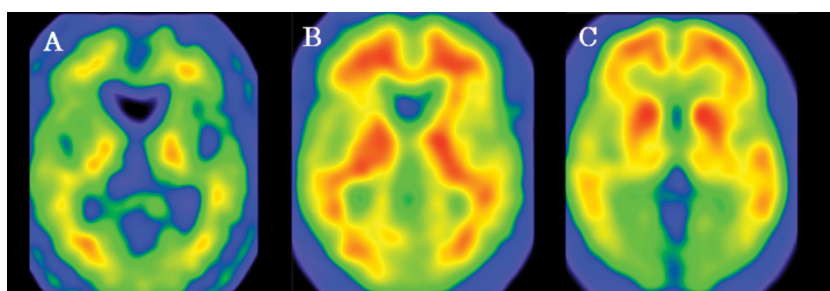


Figure 1: [¹¹C]-PiB PET examples for PiBNEG (A), STRNEG (B) and STRPOS (C) readings.

uptake values were compared with covariates of the cerebellar cortical PiB uptake values. Voxel-by-voxel statistical analysis was conducted in SPM8 using ANOVA comparisons of FDG activity and PiB uptake between the three groups: STR_{POS}, STR_{NEG} and PiB_{NEG}. Talairach Client software (Talairach Client, Research Imaging Institute of the University of Texas Health Science Center, San Antonio, Texas, USA) was used to transform MNI coordinates to Talairach coordinates [21,22].

Statistical analysis

A Student's *t*-test was performed to compare PiB and FDG uptake between STR_{POS} and STR_{NEG} groups. One-way analysis of variance and post hoc Tukey–Kramer tests were used to assess differences in SUVRs between the STR_{POS}, STR_{NEG} and PiB_{NEG} groups. The relationship between SUVR and MMSE was assessed using Pearson's correlation. Data are presented as the mean ± standard deviation or number, unless otherwise stated. For all statistical tests, *p*-values <0.05 were considered as being significant. For voxel-wise analysis with SPM, a significance threshold of *p*<0.05 family-wise error corrected was applied.

Results

Subjects characteristics of each group

As shown in Table 1, 80/141 (57%) subjects showed elevated PiB uptake in cortical areas and were visually classified as PiB positive, while 61/141 (43%) subjects did not show cortical PiB accumulation exceeding white matter uptake and were rated as PiB negative (PiB_{NEG}). Within the PiB positive group, 69/80 (86%) subjects were rated as striatal positive (STR_{POS}) according to the visual read-out, and 11 (14%) subjects were classified as striatal negative (STR_{NEG}). Among the STR_{POS} subjects, 38 were clinically diagnosed with AD, 26 with MCI due to AD, 4 with DLB, and one with SCI. The STR_{NEG} group consisted of 10 MCI patients (8 due to AD, 2 due to DLB) and one AD patient.

SUVRs of each group

Comparison of the mean cortical SUVRs revealed that the STR_{POS}

| | STR _{POS} | STR _{NEG} | PiB _{NEG} | ALL |
|-------------------------------|--------------------|--------------------|--------------------|-------------|
| <i>N</i> | 69 | 11 | 61 | 141 |
| Age (years) | 71.5 ± 8.6 | 78.5 ± 5.4 | 67.0 ± 10.6 | 70.1 ± 9.8 |
| Gender (female/male) | 25/44 | 5/6 | 35/26 | 71/69 |
| Mini-Mental State Examination | 21.6 ± 4.9 | 23.9 ± 3.3 | 25.6 ± 3.6 | 23.3 ± 4.9 |
| [¹¹ C]-PiB SUVR | 2.00 ± 0.44 | 1.46 ± 0.23 | 0.99 ± 0.19 | 1.52 ± 0.59 |
| AD | 38 | 1 | 6 | 45 |
| MCI due to AD | 26 | 8 | 0 | 34 |
| MCI due to DLB | 0 | 2 | 1 | 3 |
| MCI undefined | 0 | 0 | 23 | 23 |
| DLB | 4 | 0 | 7 | 11 |
| FTD | 0 | 0 | 7 | 7 |
| Other Dementia | 0 | 0 | 2 | 2 |
| SCI | 1 | 0 | 11 | 12 |
| Alcoholism | 0 | 0 | 1 | 1 |
| Depression | 0 | 0 | 1 | 1 |
| Epilepsy | 0 | 0 | 1 | 1 |

[¹¹C]-PiB SUVR=Averaged standardised uptake value ratio for [¹¹C]-Pittsburgh Compound-B for composite cortex regions (frontal, parieto-temporal, precuneus/posterior cingulate), referenced to cerebellar cortex; AD=Alzheimer's Disease; MCI=Mild Cognitive Impairment; DLB=Dementia with Lewy Bodies; FTD=Frontotemporal Lobar Degeneration; SCI=Subjective Cognitive Impairment; STR_{POS}=[¹¹C]-PiB-positive subjects with elevated striatal uptake; STR_{NEG}=[¹¹C]-PiB-positive subjects without elevated striatal uptake; PiB_{NEG}=[¹¹C]-PiB-negative subjects

Table 1: Demographics and clinical characteristics.

subjects showed the highest PiB accumulation, while PiB_{NEG} subjects showed the lowest (2.00 ± 0.44 for STR_{POS}, 1.46 ± 0.23 for STR_{NEG}, and 0.99 ± 0.19 for PiB_{NEG}). The differences were significant between all three groups (*p*<0.001; Figure 2). Within the PiB-positive subjects (STR_{POS} and STR_{NEG}), a positive correlation was found between cortical and striatal PiB-uptake (*r*=0.911, *p*<0.01; Figure 3).

Voxel-based analysis of PiB and FDG accumulation

Voxel-wise ANOVA comparisons in SPM revealed differences in PiB distribution between the STR_{POS} and STR_{NEG} groups, with a higher striatal uptake linked to significantly elevated PiB levels, especially in parts of the frontal and temporal cortices. The strongest correlation with striatal uptake (after uptake in the putamen, which was part of the striatal VOI) was seen in the right rectal gyrus, corresponding to Brodmann Area (BA) 11 (*P*<0.05 FWE corrected, *T*=5.89), with the MNI coordinates of the peak-level voxel being *x*=2, *y*=26, *z*=-20 (Figure 4). Other areas with PiB uptake that correlated significantly with striatal uptake included the left middle temporal gyrus, both superior temporal gyri, both inferior and superior frontal gyri, the left precuneus and posterior cingulate, left inferior parietal lobule, and the right inferior temporal gyrus (Table 2). The most significant differences in PiB uptake between the STR_{POS} and PiB_{NEG} groups were seen in the frontal cortex and the cuneal/precuneal area, with higher uptake occurring in the STR_{POS} subjects. Comparisons of the STR_{NEG} and PiB_{NEG} groups revealed that the parietal, frontal, and insular cortices showed higher

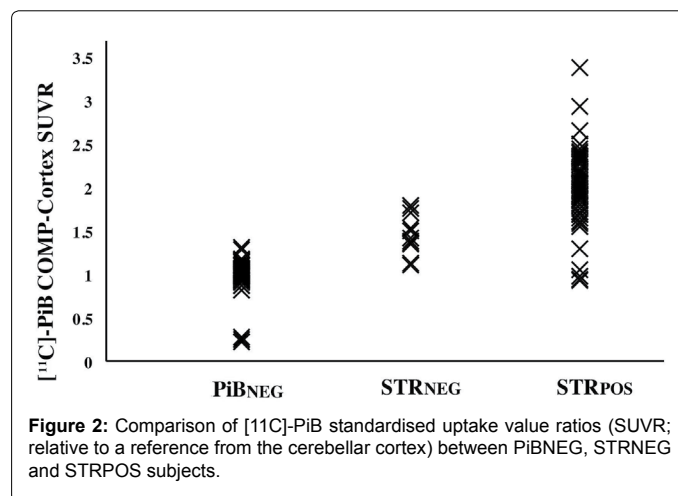


Figure 2: Comparison of [¹¹C]-PiB standardised uptake value ratios (SUVR; relative to a reference from the cerebellar cortex) between PiBNEG, STRNEG and STRPOS subjects.

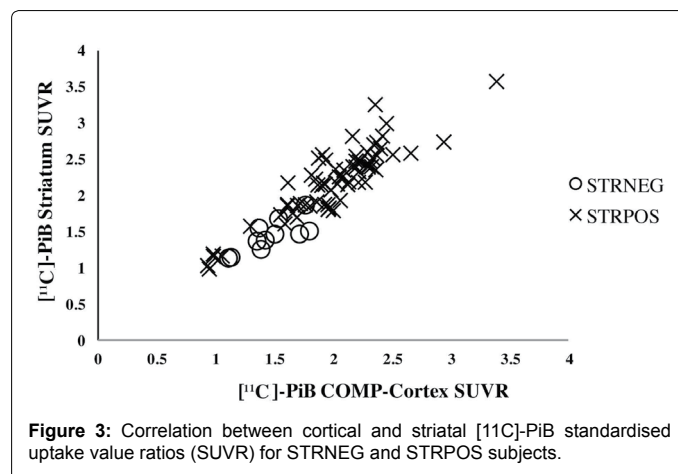


Figure 3: Correlation between cortical and striatal [¹¹C]-PiB standardised uptake value ratios (SUVR) for STRNEG and STRPOS subjects.

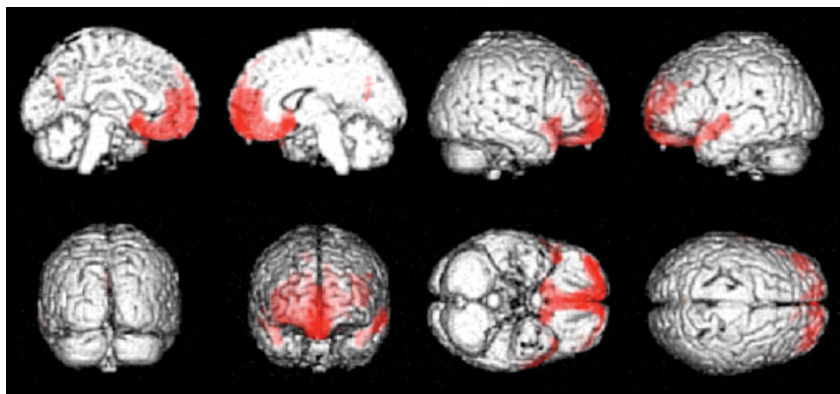


Figure 4: Brain regions with significantly higher [¹¹C]-PiB uptake in STRPOS than STRNEG subjects; p<0.05, FWE corrected.

| Comparison | Location (Brodmann Area) | t-value | x | y | z |
|---|---------------------------------|---------|-----|-----|-----|
| [¹¹ C]-PiB PET STR _{POS} >STR _{NEG} | L Putamen | 6.22 | -14 | 12 | -8 |
| | R Putamen | 6.17 | 16 | 14 | -6 |
| | R Rectal Gyrus (11) | 5.89 | 2 | 26 | -20 |
| | L Middle Temporal Gyrus (21) | 4.86 | -54 | 6 | -14 |
| | L Superior Temporal Gyrus (38) | 4.84 | -40 | 22 | -28 |
| | R Inferior Frontal Gyrus (47) | 4.80 | 46 | 20 | -8 |
| | R Superior Temporal Gyrus (38) | 4.67 | 44 | 22 | -30 |
| | R Superior Frontal Gyrus (8) | 4.46 | 12 | 44 | 50 |
| | L Precuneus (31) | 4.39 | -2 | -66 | 28 |
| | L Posterior Cingulate (31) | 4.26 | 8 | -64 | 14 |
| | L Inferior Frontal Gyrus (47) | 4.25 | -38 | 20 | -10 |
| | L Superior Frontal Gyrus (8) | 4.23 | -20 | 46 | 44 |
| | L Inferior Parietal Lobule (40) | 4.22 | -64 | -28 | 40 |
| | R Inferior Temporal Gyrus (20) | 4.17 | 50 | -20 | -38 |
| | L Middle Temporal Gyrus (39) | 4.16 | -54 | -72 | 22 |
| [¹¹ C]-PiB PET STR _{POS} >PiB _{NEG} | L Medial Frontal Gyrus (11) | 21.28 | 0 | 34 | -18 |
| | L Cuneus (7) | 19.80 | -2 | -66 | 32 |
| | L Precuneus (7) | 19.95 | -2 | -54 | 38 |
| [¹¹ C]-PiB PET STR _{NEG} >PiB _{NEG} | R Superior Parietal Lobule (7) | 7.02 | 40 | -62 | 52 |
| | L Superior Parietal Lobule (7) | 5.96 | -38 | -56 | 48 |
| | R Inferior Frontal Gyrus (9) | 4.77 | 54 | 8 | 30 |
| | L Postcentral Gyrus (5) | 4.52 | -28 | -46 | 70 |
| | L Insula | 4.43 | -36 | 16 | 2 |
| | R Precentral Gyrus (6) | 4.26 | 50 | -4 | 56 |
| | R Middle Frontal Gyrus (6) | 4.25 | 32 | -2 | 64 |
| | R Insula | 4.16 | 40 | 18 | 4 |

[¹¹C]-PiB PET=11C-Pittsburg Compound-B positron emission tomography; STRPOS=[¹¹C]-PiB-positive subjects with elevated striatal uptake; STRNEG=11C-PiB-positive subjects without elevated striatal uptake; PiBNEG=[¹¹C]-PiB-negative subjects; x=distance (mm) right (+) or left (-) of the midsagittal line; y=distance anterior (+) or posterior (-) of a vertical plane through the anterior commissure; z=distance above (+) or below (-) the inter-commissural line; L=Left; R=Right. The coordinates are in mm, relative to the anterior commissure, and correspond to the atlas of Talairach and Tournoux

Table 2: Peak locations of significant differences in [¹¹C]-PiB uptake between STR_{POS}, STR_{NEG} and PiB_{NEG} groups.

PiB binding in the STR_{NEG} group (Table 2). By contrast, the distribution pattern of FDG in the STR_{POS} and STR_{NEG} groups showed no significant regional differences.

Correlations between MMSE scores and PiB accumulations

With regard to the MMSE, the STR_{POS} group showed the lowest scores, but they were not significantly different to those from the STR_{NEG} group, with only the PiB_{NEG} group showing a significant difference to both the PiB positive groups (21.6 ± 4.9 for STR_{POS}, 23.9 ± 3.3 for STR_{NEG} and 26.6 ± 3.6 for PiB_{NEG}). Correspondingly, a negative

correlation between MMSE and cortical PiB binding (meaning a poorer cognitive performance corresponded with a higher PiB uptake) was only found when all 141 PiB positive and negative subjects were observed ($r=-0.322$, $p<0.01$), not within the 80 PiB positive subjects.

Discussion

Our study showed that in PiB positive subjects, those with an elevated striatal PiB uptake tended to have a higher mean cortical SUVR in comparison to those without elevated striatal uptake. As β -amyloid accumulation increases with time in AD [23], this finding

suggests that striatal accumulation may have occurred in the later progress of the disease in the cases we observed. This is also in accord with our finding that poorer cognitive performance (measured by MMSE) was related to a higher PiB uptake. Thal et al. observed that amyloid deposition in brains with β -amyloidosis follows a specific order, with the different areas being affected in a certain sequence. They concluded that this particular sequence was determined by a higher susceptibility to amyloidosis in certain brain regions. The striatum (which receives input from the neocortex), cingulate cortex, and parabrachial nuclei exhibit amyloid deposition only in a more advanced phase of amyloidosis [14]. By contrast, in familial forms of AD, such as presenilin-1 mutations, amyloid-precursor-protein mutations, and variant AD [24-27], increased PiB uptake in the striatum seems to be a distinct and early feature in the progression of the disease, although less cortical uptake is observed. In an investigation into differences between sporadic and familial forms of AD, Shinohara et al. suggested that amyloid deposition occurring predominantly in cortical regions in sporadic AD may be influenced by synaptic processes, while in familial forms, amyloid deposition in subcortical areas such as the striata may be mediated by effects of the amyloid precursor protein and its processing [28]. Tentolouris-Piperas et al. also reviewed amyloid PET imaging of striatal involvement in familial and sporadic AD and considered that it is unclear whether other regions develop amyloid deposits earlier in sporadic AD because there are no PET studies at the preclinical sporadic AD stages [29].

The progression of amyloid-deposition in the brain happens neither randomly nor homogeneously, but follows a distinct pattern determined by anatomical and functional neuronal connections. Beach et al. [30] investigated the correlation between the presence of histopathologically-demonstrated striatal A β deposits and visually positive ¹⁸F-flutemetamol striatal PET accumulations in 68 subjects and found the sensitivity of ¹⁸F-flutemetamol striatal PET 69%-87% and the specificity ranged between 96%-100%, then reported amyloid PET has reasonable accuracy for the detection of histologically-demonstrated striatal A β plaques.

In an examination of the association between striatal and cortical amyloid load, Ishibashi et al. found the highest correlation to occur between the ventral striatum and the medial part of the orbitofrontal area (equivalent to BA 11 and 12) [31]. Similarly, when we compared the STR_{NEG} and STR_{POS} groups, we observed the highest correlation between striatal and cortical amyloid accumulation in the right rectal gyrus (BA 11), which shows strong functional connections to the ventral portion of the striatum. The striatum is essential for decision-making [32]. As not only the striatum, but also the orbitofrontal cortex plays a major role in decision making [33] may demonstrate the relationship between striatum and basal frontal cortices. Other regions showing a positive correlation in PiB uptake with the striatal area were adjacent regions located mostly in the temporal cortex (BA 21, 38, 20, 39), as well as in other frontal areas (BA 47, 8). For all of these regions except BA 38, Di Martino et al. found positive functional connectivity relationships with striatal or dorsal caudate seed regions [34].

While we observed a positive correlation between striatal and global PiB uptake, no significant correlation was observed between striatal uptake and any regional FDG uptake within the PiB positive subjects. Similarly, Furst et al. did not find region-to-region or within region correlations between PiB and FDG PET when observing amyloid-positive subjects [35]. This may be due to the fact that amyloid accumulation does not start at the same time as neuronal degeneration and metabolic decreases in the brain (represented by the FDG uptake),

but rather several years earlier, seemingly initiating the process of neuro-degeneration [11,12,36,37]. Moreover, amyloid accumulation appears to reach a plateau level during the progression of AD, with the longitudinal PiB PET therefore changing only a little over time, while FDG accumulation depicting glucose metabolism decreases continuously [35]. Postmortem regional neurofibrillary tangle densities, but not senile plaque densities, appear to be related to regional cerebral metabolic rates for glucose metabolism in AD [38].

We found a significant negative correlation between cognitive performance and amyloid accumulation when all 141 amyloid positive and negative subjects were observed, with STR_{POS} subjects having the lowest MMSE score in cognitive testing, and PiB_{NEG} subjects having the highest score. However, this correlation did not reach a significant level when only the STR_{POS} and STR_{NEG} amyloid positive subjects were compared. This may be because the progression of a biomarker such as PET measured amyloid does not show a linear increase over time, but rather has a sigmoid trajectory that reaches a plateau in the course of AD, while cognition decreases continuously [39]. The PiB positive cases we examined in our study may have reached this plateau of amyloid accumulation, and therefore did not exhibit a further correlation between amyloid accumulation and cognitive decline represented by the MMSE. At the same time, while there was a general association between higher amyloid accumulation and greater cognitive impairment, some non-demented subjects showed an elevated level of cortical amyloid, similar to the AD patients. A given level of amyloid accumulation does not necessarily equate to a certain degree of cognitive impairment in an individual [40-42]. Epidemiologic evidence suggests that cognitive vulnerability towards the amyloid-related damages occurring in AD is affected by the individual's brain resiliency and cognitive reserves, with high IQ, being cognitively challenged at work and in leisure time, and high levels of education, being protective factors [43,44].

It is also reported that PiB binds alpha-synuclein and Lewy bodies that accumulate in the striatum in Lewy body disease brain [45]. However, the volume of accumulation is a minimum and it does not affect the SUVR or visual assessment of each subject. Our subjects included 4 DLB patients in the STR_{POS} group and they showed higher cortical PiB uptake than striatal PiB uptake.

Conclusion

Our findings demonstrated that subjects with striatal PiB uptake show higher overall cortical amyloid levels in comparison to those PiB-positive subjects without elevated striatal PiB levels, which is conclusive with striatal amyloid accumulation occurring later in the course of AD. High striatal PiB uptake is associated with higher orbitofrontal uptake, while there is no regional correlation with brain glucose metabolism measured by FDG-PET.

Compliance with Ethical Standards

Funding

This study was funded in part by Japan Society for the Promotion of Science KAKENHI Grant Number 50534103 and the 21st Century Research and Development Incentive Wages at Kindai University.

Conflict of interest

All authors of this study declare that they have no conflict of interest.

Ethical approval

All procedures performed in studies involving human participants

were in accordance with the ethical standards of the institutional and/or national research committee and with the 1964 Helsinki declaration and its later amendments or comparable ethical standards.

Informed consent

Informed consent was obtained from all individual participants or guardians included in the study.

References

1. Dharmarajan TS, Gunturu SG (2009) Alzheimer's disease: A healthcare burden of epidemic proportion. *Am Health Drug Benefits* 2: 39-47.
2. Wimo A, Winblad B, Aguero-Torres H, von Strauss E (2003) The magnitude of dementia occurrence in the world. *Alzheimer Dis Assoc Disord* 17: 63-67.
3. McKhann GM, Knopman DS, Chertkow H, Hyman BT, Jack CR, et al. (2011) The diagnosis of dementia due to Alzheimer's disease: Recommendations from the National Institute on Aging-Alzheimer's Association workgroups on diagnostic guidelines for Alzheimer's disease. *Alzheimers Dement* 7: 263-269.
4. Sperling RA, Aisen PS, Beckett LA, Bennett DA, Craft S, et al. (2011) Toward defining the preclinical stages of Alzheimer's disease: Recommendations from the National Institute on Aging-Alzheimer's Association workgroups on diagnostic guidelines for Alzheimer's disease. *Alzheimers Dement* 7: 280-292.
5. Driscoll I, Troncoso JC, Rudow G, Sojkova J, Pletnikova O, et al. (2012) Correspondence between *in vivo* (11C)-PiB-PET amyloid imaging and post-mortem, region-matched assessment of plaques. *Acta Neuropathol* 124: 823-831.
6. Ikonomic MD, Klunk WE, Abrahamson EE, Mathis CA, Price JC, et al. (2008) Post-mortem correlates of *in vivo* PiB-PET amyloid imaging in a typical case of Alzheimer's disease. *Brain* 131: 1630-1645.
7. Klunk WE, Wang Y, Huang GF, Debnath ML, Holt DP, et al. (2001) Uncharged thioflavin-T derivatives bind to amyloid-beta protein with high affinity and readily enter the brain. *Life Sci* 69: 1471-1484.
8. Leinonen V, Rinne JO, Virtanen KA, Eskola O, Rummukainen J, et al. (2013) Positron emission tomography with [18F]flutemetamol and [11C]PiB for *in vivo* detection of cerebral cortical amyloid in normal pressure hydrocephalus patients. *Eur J Neurol* 20:1043-1052.
9. Rowe CC, Ng S, Ackermann U, Gong SJ, Pike K, et al. (2007) Imaging beta-amyloid burden in aging and dementia. *Neurology* 68: 1718-1725.
10. Braak H, Braak E (1991) Neuropathological staging of Alzheimer-related changes. *Acta Neuropathol* 82: 239-259.
11. Jack CR, Knopman DS, Jagust WJ, Petersen RC, Weiner MW, et al. (2013) Tracking pathophysiological processes in Alzheimer's disease: An updated hypothetical model of dynamic biomarkers. *Lancet Neurol* 12: 207-216.
12. Jack CR, Knopman DS, Jagust WJ, Shaw LM, Aisen PS, et al. (2010) Hypothetical model of dynamic biomarkers of the Alzheimer's pathological cascade. *Lancet Neurol* 9: 119-128.
13. Braak H, Braak E (1997) Frequency of stages of Alzheimer-related lesions in different age categories. *Neurobiol Aging* 18: 351-357.
14. Thal DR, Rüb U, Orantes M, Braak H (2002) Phases of a beta-deposition in the human brain and its relevance for the development of AD. *Neurology* 58: 1791-1800.
15. McKhann G, Drachman D, Folstein M, Katzman R, Price D, et al. (1984) Clinical diagnosis of Alzheimer's disease: Report of the NINCDS-ADRDA Work Group under the auspices of Department of Health and Human Services Task Force on Alzheimer's disease. *Neurology* 34: 939-944.
16. McKeith IG, Dickson DW, Lowe J, Emre M, O'Brien JT, et al. (2005) Diagnosis and management of dementia with Lewy bodies: Third report of the DLB Consortium. *Neurology* 65: 1863-1872.
17. Neary D, Snowden JS, Gustafson L, Passant U, Stuss D, et al. (1998) Frontotemporal lobar degeneration: A consensus on clinical diagnostic criteria. *Neurology* 51: 1546-1554.
18. Petersen RC, Doody R, Kurz A, Mohs RC, Morris JC, et al. (2001) Current concepts in mild cognitive impairment. *Arch Neurol* 58: 1985-1992.
19. Hosokawa C, Ishii K, Hyodo T, Sakaguchi K, Usami K, et al. (2015) Investigation of (11C)-PiB equivocal PET findings. *Ann Nucl Med* 29: 164-169.
20. Fodero-Tavoletti MT, Rowe CC, McLean CA, Leone L, Li QX, et al. (2009) Characterization of PiB binding to white matter in Alzheimer disease and other dementias. *J Nucl Med* 50: 198-204.
21. Lancaster JL, Rainey LH, Summerlin JL, Freitas CS, Fox PT, et al. (1997) Automated labeling of the human brain: A preliminary report on the development and evaluation of a forward-transform method. *Hum Brain Mapp* 5: 238-242.
22. Lancaster JL, Woldorff MG, Parsons LM, Liotti M, Freitas CS, et al. (2000) Automated Talairach atlas labels for functional brain mapping. *Hum Brain Mapp* 10: 120-131.
23. Jack CR, Lowe VJ, Weigand SD, Wiste HJ, Senjem ML, et al. (2009) Serial PiB and MRI in normal, mild cognitive impairment and Alzheimer's disease: implications for sequence of pathological events in Alzheimer's disease. *Brain* 132: 1355-1365.
24. Klunk WE, Price JC, Mathis CA, Tsopelas ND, Lopresti BJ, et al. (2007) Amyloid deposition begins in the striatum of presenilin-1 mutation carriers from two unrelated pedigrees. *J Neurosci* 27: 6174-6184.
25. Koivunen J, Verkkoniemi A, Aalto S, Paetau A, Ahonen JP, et al. (2008) PET amyloid ligand [11C]PiB uptake shows predominantly striatal increase in variant Alzheimer's disease. *Brain* 131: 1845-1853.
26. Remes AM, Laru L, Tuominen H, Aalto S, Kempainen N, et al. (2008) Carbon 11-labeled pittsburgh compound B positron emission tomographic amyloid imaging in patients with APP locus duplication. *Arch Neurol* 65: 540-544.
27. Villemagne VL, Ataka S, Mizuno T, Brooks WS, Wada Y, et al. (2009) High striatal amyloid beta-peptide deposition across different autosomal Alzheimer disease mutation types. *Arch Neurol* 66: 1537-1544.
28. Shinohara M, Fujioka S, Murray ME, Wojtas A, Baker M, et al. (2014) Regional distribution of synaptic markers and APP correlate with distinct clinicopathological features in sporadic and familial Alzheimer's disease. *Brain* 137: 1533-1549.
29. Tentolouris-Piperas V, Ryan NS, Thomas DL, Kinnunen KM (2017) Brain imaging evidence of early involvement of subcortical regions in familial and sporadic Alzheimer's disease. *Brain Res* 1655: 23-32.
30. Beach TG, Thal DR, Zhanette M, Smith A, Buckley C (2016) Detection of Striatal Amyloid Plaques with [18F]flutemetamol: Validation with post-mortem histopathology. *J Alzheimers Dis* 52: 863-873.
31. Ishibashi K, Ishiwata K, Toyohara J, Murayama S, Ishii K (2014) Regional analysis of striatal and cortical amyloid deposition in patients with Alzheimer's disease. *Eur J Neurosci* 40: 2701-2706.
32. Burton AC, Bissonette GB, Lichtenberg NT, Kashteyan V, Roesch MR (2014) Ventral striatum lesions enhance stimulus and response encoding in dorsal striatum. *Biol Psychiatry* 75: 132-139.
33. Wallis JD (2007) Orbitofrontal cortex and its contribution to decision-making. *Annu Rev Neurosci* 30: 31-56.
34. Di Martino A, Scheres A, Margulies DS, Kelly AM, Uddin LQ, et al. (2008) Functional connectivity of human striatum: A resting state fMRI study. *Cereb Cortex* 18: 2735-2747.
35. Forster S, Grimmer T, Miederer I, Henriksen G, Yousefi BH, et al. (2012) Regional expansion of hypometabolism in Alzheimer's disease follows amyloid deposition with temporal delay. *Biol Psychiatry* 71: 792-797.
36. Lo RY, Hubbard AE, Shaw LM, Trojanowski JQ, Petersen RC, et al. (2011) Longitudinal change of biomarkers in cognitive decline. *Arch Neurol* 68: 1257-1266.
37. Morris JC, Price JL (2001) Pathologic correlates of nondemented aging, mild cognitive impairment, and early-stage Alzheimer's disease. *J Mol Neurosci* 17: 101-118.
38. De Carli CS, Attack JR, Ball MJ, Kay JA, Grady CL, et al. (1992) Post-mortem neurofibrillary tangle densities but no senile plaque densities are related to regional metabolic rates of glucose during life in Alzheimer's disease patients. *Neurodegeneration* 1: 113-121.
39. Jack CR Jr, Wiste HJ, Lesnick TG, Weigand SD, Knopman DS, et al. (2013) Brain β -amyloid load approaches a plateau. *Neurology* 80: 890-896.
40. Jack CR Jr, Lowe VJ, Senjem ML, Weigand SD, Kemp BJ, et al. (2008) 11C PiB and structural MRI provide complementary information in imaging of

-
- Alzheimer's disease and amnesic mild cognitive impairment. *Brain* 131: 665-680.
41. Mintun MA, Larossa GN, Sheline YI, Dence CS, Lee SY, et al. (2006) [11C] PIB in a non-demented population: Potential antecedent marker of Alzheimer disease. *Neurology* 67: 446-452.
42. Schmitt FA, Davis DG, Wekstein DR, Smith CD, Ashford JW, et al. (2000) "Preclinical" AD revisited: Neuropathology of cognitively normal older adults. *Neurology* 55: 370-376.
43. Stern Y (2006) Cognitive reserve and Alzheimer disease. *Alzheimer Dis Assoc Disord* 20: 112-117.
44. Vemuri P, Weigand SD, Przybelski SA, Knopman DS, Smith GE, et al. (2011) Cognitive reserve and Alzheimer's disease biomarkers are independent determinants of cognition. *Brain* 134: 1479-1492.
45. Maetzler W, Reimold M, Liepelt I, Solbach C, Leyhe T, et al. (2008) [11C]PIB binding in Parkinson's disease dementia. *Neuroimage* 39: 1027-1033.